

1 **Increased Primary and Secondary H₂SO₄ Showing the Opposing Roles in SOA**
2 **Formation from Ethyl Methacrylate Ozonolysis**

3 Peng Zhang ^{a, c, #}, Tianzeng Chen ^{a, c, #}, Jun Liu ^{a, c}, Guangyan Xu ^{a, c}, Qingxin Ma ^{a, b, c, *},
4 Biwu Chu ^{a, b, c, *}, Wanqi Sun^d, and Hong He ^{a, b, c}

5 ^a State Key Joint Laboratory of Environment Simulation and Pollution Control,
6 Research Center for Eco-Environmental Sciences, Chinese Academy of Sciences,
7 Beijing 100085, China

8 ^b Center for Excellence in Regional Atmos. Environ., Institute of Urban Environment,
9 Chinese Academy of Sciences, Xiamen 361021, China

10 ^c University of Chinese Academy of Sciences, Beijing 100049, China

11 ^d CMA Meteorological Observation Centre, Beijing, 100081, China

12 [#] These authors contributed equally to this work

13
14
15
16
17
18
19
20
21
22
23
24
25
26
27
28
29
30

31 **Abstract**

32 Stressed plants and polymer production can emit many unsaturated volatile organic
33 esters (UVOEs). However, secondary organic aerosol (SOA) formation of UVOEs
34 remain unclear, especially under complex ambient conditions. In this study, we mainly
35 investigated ethyl methacrylate (EM) ozonolysis. Results showed that a substantial
36 increase in secondary H₂SO₄ particles promoted SOA formation with increasing SO₂.
37 An important reason was that the homogeneous nucleation of more H₂SO₄ at high SO₂
38 level provided greater surface area and volume for SOA condensation. However,
39 increased primary H₂SO₄ with seed acidity enhanced EM uptake, but reduced SOA
40 formation. This was ascribed to the fact that the ozonolysis of more adsorbed EM was
41 hampered with the formation of surface H₂SO₄ at higher particle acidity. Moreover, the
42 increase in secondary H₂SO₄ particle via homogeneous nucleation favored to the
43 oligomerization of oxidation products, whereas the increasing of primary H₂SO₄ with
44 acidity in the presence of seed tended to promote the functionalization conversion
45 products. This study indicated that the role of increased H₂SO₄ to EM-derived SOA
46 maybe not the same under different ambient conditions, which helps to advance our
47 understanding of the complicated roles of H₂SO₄ in the formation of EM-derived SOA.

48
49
50
51
52
53
54
55
56
57
58
59
60
61
62
63
64
65

66 **1. Introduction**

67 Unsaturated volatile organic esters (UVOEs) are oxygenated volatile organic
68 compounds (OVOCs) with many large-scale commercial uses. They are not only used
69 as potential replacements of traditional solvents and additive in diesel fuels but are
70 widely used in the production of polymers and resins (Colomer et al., 2013; Taccone et
71 al., 2016; Teruel et al., 2016; Wang et al., 2010). Thus, the production, processing,
72 storage, and disposal of industrial products all contribute to UVOE emissions. In
73 addition, emissions of green leaf volatiles (GLVs), a class of wound-induced OVOCs,
74 also contribute to UVOEs in the atmosphere (Arey et al., 1991; Blanco et al., 2014;
75 Hamilton et al., 2009; Konig et al., 1995). Once emitted into the atmosphere, these
76 UVOEs quickly undergo complex chemical reactions with OH radicals and ozone in
77 sunlight (Bernard et al., 2010; Blanco et al., 2010; Sun et al., 2015), NO₃ radicals during
78 night-time (Salgado et al., 2011; Wang et al., 2010), and Cl atoms in certain
79 environments (Blanco et al., 2010; Rivela et al., 2018). OH-initiated oxidation of GLVs,
80 including *cis*-3-hexenylacetate (CHA) to secondary organic aerosol (SOA), is estimated
81 to contribute 1–5 TgC/y, with up to a third of that from isoprene (Hamilton et al., 2009).
82 In addition, CHA-derived SOA is a more efficient absorber (between 190 and 900 nm)
83 than other OVOCs (such as *cis*-3-hexenol) due to the high proportion of carbonyl-
84 containing species (Harvey et al., 2016). Thus, UVOEs can be considered as a class of
85 potential SOA precursors. Further investigations on UVOE-derived SOA under
86 complex ambient conditions will help to better understand their contribution to ambient
87 aerosol.

88 Recent studies ascertained that the presence of SO₂ and sulfate seed particles all
89 have a significant impact on the yield, composition, and formation mechanism of SOA
90 (Han et al., 2016; Kristensen et al., 2014; Wong et al., 2015; Zhang et al., 2019). For
91 example, an increase in SO₂ can enhance SOA production due to the formation of more
92 sulfates and the enhanced acid-catalysis role during the atmospheric oxidation of
93 various VOCs (Chu et al., 2016; Lin et al., 2013; Zhao et al., 2018). In the presence of
94 alone seed particles, however, increased particle acidity will not always enhance SOA

95 formation and may have a negligible effect on the SOA formation(Han et al., 2016;
96 Kristensen et al., 2014; Riva et al., 2016; Surratt et al., 2010; Wong et al., 2015; Zhang
97 et al., 2019). Furthermore, it is worth noting that several studies have indicated that an
98 increase in SO₂ can promote the average oxidation state (OS_c) of SOA due to
99 organosulfate formation(Liu et al., 2019a; Shu et al., 2018; Zhang et al., 2019). Whereas
100 other studies have suggested that an increase SO₂ can have a suppression effect on SOA
101 OS_c (Friedman et al., 2016). Similarly, the effect of increased aerosol acidity on SOA
102 OS_c depends on the contribution of functionalization and oligomerization reactions to
103 SOA composition as increased aerosol acidity can promote these reactions (Shu et al.,
104 2018). This implies that the roles of increased sulfate particles and particle acidity in
105 SOA production and composition are very complicated and need to be further studied.

106 Methacrylate was one of the main effluents in the class of UVOEs. Just in China,
107 the net import of methacrylate has up to about 930 thousand tons in 2019. It was worth
108 noting that ethyl methacrylate, one of methacrylate, has been widely detected in
109 ambient air due to the wide variety of sources and high volatility (Pankow et al., 2003).
110 Moreover, some exposure measurement studies indicated that the concentration of ethyl
111 methacrylate was up to 31-108 µg m⁻³ in the salons working air, which was notably
112 higher than other methacrylate (Henriks-Eckerman and Korva, 2012). Thus, we used
113 ethyl methacrylate (EM) as an UVOE proxy to investigate the effects of different SO₂
114 levels and seed particle acidity on the formation and evolution of EM-derived SOA in
115 this work. This work will help to better understanding the formation of EM-derived
116 SOA under complex conditions.

117

118 **2 Materials and methods**

119 Multiple EM ozonolysis experiments were conducted in a 30-m³ cuboid Teflon smog
120 chamber (L × W × H = 3.0 × 2.5 × 4.0 m) under 298 K temperature and atmospheric
121 pressure. Experimental conditions are summarized in Table S1. The chamber operation,
122 analytical techniques, and experimental procedures are described in detail elsewhere
123 (Chen et al., 2019b). Only a brief description on the specific procedures relevant to this

124 work is presented here.

125 Prior to each experiment, the chamber was first inflated using purified and dry zero
126 air with a flow rate of 120 L min⁻¹ for 10 min, subsequently air pump began to run for
127 5 min. The stainless-steel fan installed at the bottom of chamber was kept to run during
128 the whole cleaning process. Prior to each experiment, Teflon chamber was repeatedly
129 and circularly cleaned by purified and dry zero air using above method for about 24 h
130 until almost no NO_x could be detected or the particle number concentration was < 30
131 cm⁻³. The cleaning procedure of chamber was consistent with that described in our
132 previous studies (Chen et al., 2019a; Liu et al., 2019a). The O₃ (generated by passing 4
133 L min⁻¹ dry zero air over two UV photochemical tubes (40-cm length and 4-cm inter-
134 diameter)), SO₂ (520 ppm in N₂, Beijing Huayuan, China), and CO (0.05% in N₂,
135 Beijing Huayuan, China) were added into the chamber in sequence. EM were first
136 added into a stainless-steel tee at 80 °C and subsequently flushed into the chamber by
137 zero gas with the flowrate of 20 L min⁻¹. We applied CO to decrease the effect of OH
138 radical reaction via scavenging of OH radicals. The EM (98% purity, Sigma-Aldrich,
139 USA) was added to the chamber by injection of a known volume into a heated three-
140 way tube (80 °C) and flushed into the chamber by dry zero air. A stainless-steel fan is
141 used to ensure homogeneous mixing of reactants.

142 To minimize losses in the sampling line, various monitoring instruments
143 surrounded and are next to the smog chamber. The length of sampling pipes of various
144 monitoring instruments ranged from 0.5-1.0 m. A scanning mobility particle sizer
145 (SMPS, TSI, Inc.), consisting of differential mobility analyzer (DMA; model 3082),
146 condensation particle counter (CPC; model 1720), and Po210 bipolar neutralizer, was
147 applied to measure number size distribution. Total particle number and mass
148 concentrations were calculated assuming a uniform density for aerosol particles of 1.4
149 g cm⁻³ (Liu et al., 2019b; Chen et al., 2019b). The sheath flow and aerosol flow in the
150 SMPS were set to 3.0 and 0.3 L min⁻¹, respectively. The SMPS results were further
151 corrected via the wall loss rate of (NH₄)₂SO₄ particles and the correction magnitude is
152 about 10% in 5 h-reaction (Figure S1). The desorption or off-gassing of organic gaseous

批注 [Peng1]: Reviewer 1: Specific comments Q2;

批注 [Peng2]: Reviewer 2: Specific comments Q1;

批注 [Peng3]: Reviewer 1: Specific comments Q4;

153 products and NH₃ from chamber wall could be absorbed by seed particles to some
154 extent during introducing seed particles. However, the influence of these particulate
155 species to newly produced secondary particles could be ignorable based on the
156 comparison of their concentrations (Figure S2).

批注 [Peng4]: Reviewer 1: Specific comments Q2;

157 Based on the different characterized fragments, both mass concentration and
158 evolution of the different chemical compositions of aerosol particles were
159 simultaneously measured online using High-Resolution Time-of-Flight Aerosol Mass
160 Spectrometric Analysis (HR-ToF-AMS; Aerodyne Research Inc., USA). The AMS
161 working principles and modes of operation are explained in detail elsewhere. According
162 to standard protocols, the inlet flow rate, ionization efficiency (IE), and particle sizing
163 were calibrated using size-selected pure ammonium nitrate (AN) particles (Drewnick
164 et al., 2005). The HR-ToF-AMS analysis toolkit SQUIRREL 1.57I/PIKA v1.16I in Igor
165 Pro v6.37 was employed to process and analyze the experimental data obtained by the
166 HR-ToF-AMS. To reduce the sampling errors resulting from calibrating HR-TOF-
167 AMS before each experiment, the HR-ToF-AMS results were further corrected using
168 mass concentration derived from the SMPS as per Gordon et al (Gordon et al., 2014).
169 A series of gas analyzers from Thermo Scientific (USA) were used to monitor the
170 evolution of SO₂ (model 43i), CO (model 48i), and O₃ (model 49i) concentrations as a
171 function of reaction time. Some recent studies indicated that higher CO levels were
172 found to significantly change the chemical composition of SOA relative to low CO level
173 (Zhang et al., 2020; McFiggans et al., 2019). Thus, about 36-38 ppm CO was added in
174 the chamber to exclude OH radical influence during each experiment. Moreover, to
175 make sure results reliable and rule out potential artifacts including the adding sequence
176 of CO, O₃, and SO₂ during experimental preparation and the injection process of EM,
177 parallel experiments (twice experiments at the same experimental conditions) under
178 selected experimental conditions (135 ppb SO₂ and in the presence of AS seeds,
179 respectively) were conducted (Figure S3 and S4).

批注 [Peng5]: Reviewer 1: Specific comments Q13;
Reviewer 2: Specific comments Q1;

180

181 3. Results and discussion

182 3.1. Overview of EM-derived SOA Formation with and without Seed Particles

183 We first investigated the ozonolysis of alone EM. As shown in Figure S5, the
184 ozonolysis of alone EM could not produce SOA in the absence of seed and SO₂.

185 Similarly, the increased particle acidity did not promote SOA formation during the
186 ozonolysis of alone EM in the absence of SO₂ (Figure S6 and S7). Thus, this study

批注 [Peng6]: Reviewer 2: Specific comments Q4;

187 mainly focused on EM ozonolysis in the presence of SO₂. Secondary particle formation
188 from EM ozonolysis with different SO₂ levels was first investigated in the absence of
189 seed particles. As shown in Figure 1, SOA and sulfate were significantly produced once
190 EM was introduced into the reaction chamber. Moreover, both SOA and sulfate

191 formation were markedly enhanced with the increase in initial SO₂ concentration
192 (Figure 1A and B). This indicated that EM-derived SOA formation was closely related
193 to sulfate formation compared with that the ozonolysis of alone EM. Subsequently, EM
194 ozonolysis with the same level of SO₂ (132-138 ppb) was also conducted in the

批注 [Peng7]: Reviewer 2: Specific comments Q6;

195 presence of seed particles with different acidity (neutral and acidic). Two different
196 solutions, including AS (0.02 mol L⁻¹) and AS + H₂SO₄ (0.02 + 0.04 mol L⁻¹), were
197 nebulized into the chamber, respectively, to provide the corresponding seed aerosol for
198 acidity experiments. The initial seed concentrations have been added in the Table S1.

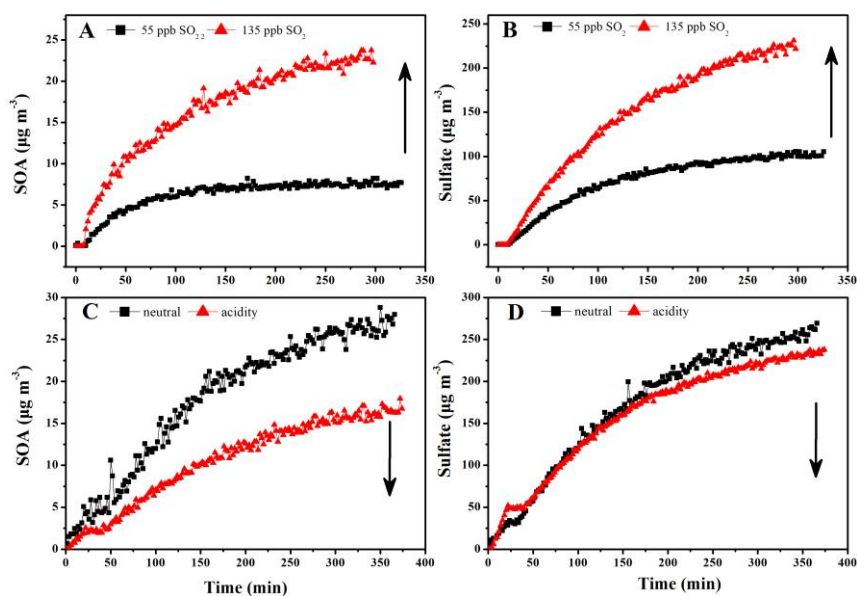
199 Interestingly, with the increase of seed acidity, the maximum mass concentrations of
200 SOA and sulfate decreased from 19.1 to 12.9 μg m⁻³ (Figure 1C) and 192.6 to 169.7 μg

批注 [Peng8]: Reviewer 2: Specific comments Q7;

201 m⁻³ (Figure 1D), respectively. This indicated that increased particle acidity reduced
202 secondary particle formation in the presence of SO₂, which was inconsistent with the
203 enhancement effect of particle acidity via acid-catalysis on SOA formation during
204 alkene photooxidation (such as isoprene, isoprene epoxydiols, and glyoxal) (Kristensen
205 et al., 2014; Lin et al., 2012; Riva et al., 2016; Wong et al., 2015). In order to evaluate
206 whether the effect is atmospherically relevant, these experiments of seed particle role
207 were also conducted at higher RH (45-50% RH). As shown in Figure S8, it could be
208 found that increased particle acidity also suppressed the formation of SOA and sulfate
209 at higher RH. Thus, these results imply that the increase of primary H₂SO₄ proportion
210 with particle acidity in seed particles and the increase of secondary H₂SO₄ particles

211 with SO₂ concentration exhibited the opposite role in EM-derived SOA formation. In
212 addition, the change in RH was found to have an impact on the formation of EM-
213 derived SOA and sulfate, consistent with our recent studies (Zhang et al., 2019; Zhang
214 et al., 2020). SOA concentration at 45% RH was reduced by a factor of 2 relative to that
215 at 10% RH in this work (Figure S9). The changes in both sulfate and SOA concentration
216 were attributed to the competitive reaction between SO₂ and H₂O toward sCI. The
217 suppression of H₂SO₄ concentration was attributed to the rapid consumption of sCI by
218 water and water dimer at high RH (42%). The suppression of SOA mass loading should
219 be ascribed to the formation of volatile organic peroxides at high RH.

批注 [Peng9]: Reviewer 2: Specific comments Q8;



220
221 **Figure 1.** Time-dependent growth curves of SOA (A) and sulfate (B) under different
222 initial concentrations of SO₂ in absence of seed particles; SOA (C) and sulfate (D) after
223 subtracting seeds in presence of neutral and acidic seed particles.

224 As shown in Figure 2, the size distributions of secondary particles under different
225 experimental conditions were also compared. The detected maximum particle
226 concentration (790 000 particle cm⁻³) under 135 ppb SO₂ was higher than that observed
227 under 55 ppb SO₂ (300 000 particle cm⁻³) in the absence of seed particles (Figure 2A
228 and B). Recent studies suggested that the reaction between SO₂ and stable Criegee

229 intermediates (sCI) dominated the formation of H₂SO₄ particles and was enhanced with
230 increased SO₂ concentration. An important reason for this is the rapid homogeneous
231 nucleation of H₂SO₄ not only can provide greater surface area and volume for the
232 condensation of low-volatile products, but reduce the fraction of these semi-volatile
233 species lost to the wall (Chu et al., 2016; Liu et al., 2017; Zhang et al., 2019; Zhang et
234 al., 2014). The high PToF size of sulfate and surface concentration of fine particles at
235 high SO₂ level supported above conclusion (Figure S10 and S11). In the presence of
236 seed particles, we used similar average concentration (~25 000-30000 particles cm⁻³)
237 under different acidities to reduce the disturbance of seed particle concentration (Figure
238 2C and 2D). The mean size and surface concentration of acidified AS (AAS) was
239 higher than AS (Figure S11B). Results showed ~300 000 newly produced particles cm⁻³
240 for neutral AS seeds (Figure 2C) and ~74 000 newly produced particles cm⁻³ for
241 acidified AS seeds (Figure 2D), respectively. The reduction of NPF in the presence of
242 acidic particles most likely result from that acidic seed particles with high mean size
243 and surface concentration promoted the condensation of gaseous nucleation species
244 onto seed surface. However, this could not explain why both SOA and sulfate were all
245 suppressed with the increase in particle acidity. Thus, one reasonable explanation is that
246 acidic seed particles also enhanced EM uptake on the particle surface as well as
247 promoting the condensation of nucleation species. As a result, the heterogeneous
248 formation of fresher H₂SO₄ on the surface of seed particles subsequently reduced SOA
249 formation by hampering the ozonolysis of adsorbed EM. To further supported this
250 speculation, we first investigated the EM uptake on different using a gas mass
251 spectrometer (QMS, GAM 200, Bremen, Germany). As shown in Figure S12, the
252 increase in H₂SO₄ concentration indeed promoted the uptake of EM on seed particle
253 with the increase of acidity. To further verify the presence of SO₂ could hamper the
254 ozonolysis of adsorbed EM due to surface H₂SO₄ formation, we checked and compared
255 the degradation of adsorbed EM during its ozonolysis in the absence and presence of
256 SO₂ using the in situ attenuated total internal reflection infrared (ATR-IR) spectra. As
257 shown in Figure S13, it could be found that EM consumption in the presence of SO₂

批注 [Peng10]: Reviewer 2: Specific comments Q2 and Q5;

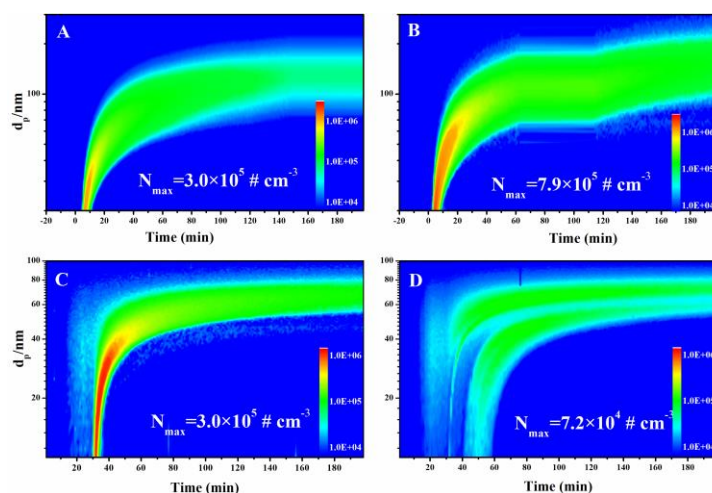
批注 [Peng11]: Reviewer 2: Specific comments Q2 and Q5;

258 was slower than that in the absence of SO₂. This indicated that higher particle acidity
259 indeed promoted EM uptake on the particle surface and the presence of SO₂ resulted in
260 the residual of more adsorbed EM on particle surface.

批注 [Peng12]: Reviewer 2: Specific comments Q9;

261 In addition, as shown in Figure S5 and S6, the negligible change of SOA with
262 acidity in the absence of SO₂ also supported that the reducing effect of increasing
263 particle acidity on secondary particle formation was closely related to the formation of
264 H₂SO₄ particles in the presence of SO₂. And some recent studies proved that the
265 presence of inorganic acids HCl can may also be an effective scavenger of sCI, further
266 suppressing the formation of low-volatility oligomers (SOA composition) (Zhao et al.,
267 2015). The reaction between sCI and HNO₃ or HCl in particularly was likely to be an
268 important sink of sCI in polluted urban areas under dry conditions (Foreman et al.,
269 2016). Thus, we speculated that the surface secondary reactions between sCI and H₂SO₄
270 under acidity condition may also suppress the formation of low-volatility oligomers via
271 affecting the sCI lifetime like HCl or HNO₃. Taken together, these results imply that
272 the SOA formation under different SO₂ levels and different particle acidities may be
273 closely related to the homogeneous or heterogeneous formation of H₂SO₄.

批注 [Peng13]: Reviewer 2: Specific comments Q10;
Reviewer 1: Specific comments Q6;



274
275 **Figure 2.** Size distribution of secondary aerosol as a function of time at 55 ppb SO₂ (A)
276 and 135 ppb SO₂ (B) and under AS seed particle (C) and Acidic AAS seed particle (D).
277

278 3.2. Chemical Interpretation and Elemental Analysis of SOA

279 Recent studies have suggested that a higher proportion of H₂SO₄ in aerosol can
280 result in greater formation of oligomers and high-oxygenated organic aerosol via
281 acceleration of the acid-catalysis process (Inuma et al., 2004; Kristensen et al., 2014;
282 Liu et al., 2019a; Rodigast et al., 2017; Shu et al., 2018; Zhang et al., 2019). In order
283 to make clear whether the homogeneous or heterogeneous formation of H₂SO₄ could
284 also affect SOA composition, we further analyze SOA composition and evolution based
285 on positive matrix factorization (PMF) solution and Van Krevelen diagrams (Ulbrich
286 et al., 2009; Zhang et al., 2005). The methodological of PMF analysis has been put into
287 Supporting Information (Figure S14 and S15). The time series and mass spectra of each
288 Factor after PMF analysis were applied to characterize the factor constitution and
289 chemical conversion among factors (Ulbrich et al., 2009; Zhang et al., 2005).

批注 [Peng14]: Reviewer 1: Specific comments Q8;

290 *Positive matrix factorization (PMF) solution*

291 In the absence of seed particles, two factors were identified under different SO₂
292 concentrations. As shown in Figure 3A, the 43 (C₂H₃O⁺) higher signals (tracers for
293 alcohols and aldehydes) and prominent fragmental peaks containing one-oxygen atom
294 (i.e., C₂H₄O, C₂H₅O, C₃H₅O, C₃H₅O, C₃H₇O, C₄HO, and C₆H₁₀O) observed in Factor
295 2 implied that Factor 2 consisted of less-oxygenated organic aerosols. The 44 (CO₂⁺)
296 higher signals, tracers for organic acids, and dominant peaks containing multi-oxygen
297 atoms (i.e., C₃H₈O₃, C₃H₉O₃, and C₄H₁₀O₃) observed in Factor 1 implied that Factor 1
298 consisted of more-oxygenated organic aerosols. From the temporal variations in Figure
299 3B, both Factor 1 and 2 continuously increased with reaction progress before 200 min.
300 This implied that both Factors were simultaneously produced and SOA growth should
301 be mainly attributed to the adsorption and condensation of both less oxidized species
302 and more oxidized species on particle before 200 min. After 200 min, Factor 1
303 continuously increased but Factor 2 decreased, suggesting that the chemical conversion
304 of part of less-oxygenated species in Factor 2 to more-oxygenated products in Factor 1
305 in the latter period of reaction. Moreover, the average elemental compositions of Factor
306 1 and Factor 2 were estimated to be C_{2.29}H₃O_{0.53}S_{0.01} and C_{1.38}H_{1.87}O_{0.37}S_{0.027},

批注 [Peng15]: Reviewer 2: Specific comments Q12;

批注 [Peng16]: Reviewer 1: Specific comments Q9;
Reviewer 2: Specific comments Q12;

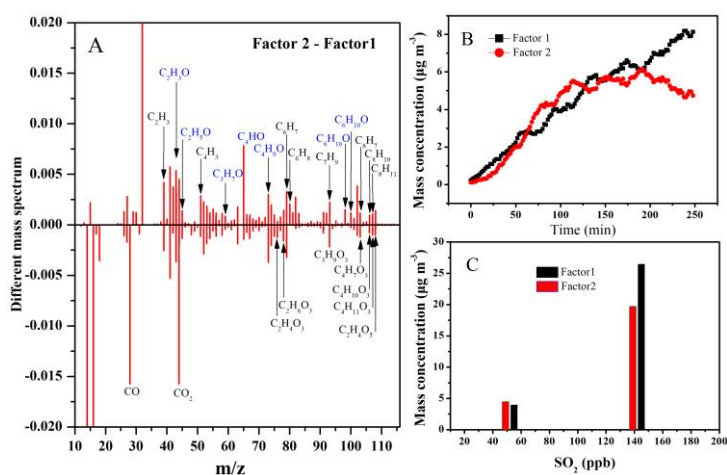
批注 [Peng17]: Reviewer 1: Specific comments Q1 and Q9;

307 respectively. Higher OS_c of Factor 2 (-0.85) relative to that Factor 1 (-0.81) also
 308 supported above conclusion. This also implied that the acid-catalyzed role could
 309 promote the chemical conversion from Factor 2 to Factor 1 when the H_2SO_4 proportion
 310 (acidity) in the particle-phase reached a certain concentration (Liu et al., 2019a;
 311 Offenberg et al., 2009). The evolution of org 43 and org 44 fragments, representing the
 312 characterized fragment of low-and high-oxidized species, further supported above
 313 conclusion (Figure S16). As shown in Figure 3C, the maximum production of both
 314 Factor 1 and Factor 2 increased with increasing SO_2 . One reasonable explanation is that
 315 the formation of more H_2SO_4 particles with increasing SO_2 provided a greater surface
 316 area and volume for the simultaneous condensation of both less-oxygenated and more-
 317 oxygenated organic products (Chu et al., 2016; Liu et al., 2017; Zhang et al., 2019).

批注 [Peng18]: Reviewer 1: Specific comments Q9;
 Reviewer 2: Specific comments Q12;

批注 [Peng19]: Reviewer 1: Specific comments Q9;
 Reviewer 2: Specific comments Q12;

批注 [Peng20]: Reviewer 1: Specific comments Q1 and Q9;

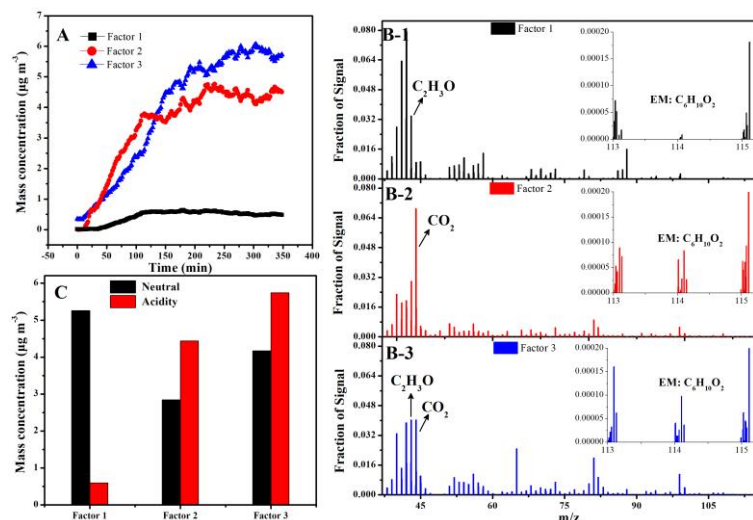


318
 319 **Figure 3.** Two-factor solutions for PMF analyses of SOA under different SO_2
 320 concentrations: (A) Different mass spectra between two factors (Factor 2-Factor 1) at
 321 135 ppb SO_2 ; (B) Time series of factor concentrations; (C) Maximum concentration of
 322 two factors at 55 ppb and 135 ppb SO_2 .

323 In the presence of seed particles, the chemical evolution of SOA components under
 324 different acidity conditions was also compared based on PMF analysis. From the
 325 temporal variations in Figure 4A, three factors were identified and almost
 326 simultaneously increased. Based on the mass spectra of the three factors (Figure 4B),

327 the fragments containing less-oxygenated species in Factor 1 (such as typical fragment
328 $C_2H_3O^+$ (m/z 43)) were more abundant than in Factor 2. In contrast, the fragments
329 containing more-oxygenated species in Factor 2 (such as typical fragment CO_2^+ (m/z
330 44)) were more abundant than in Factor 1. Thus, Factor 1 and 2 were tentatively
331 assigned to less-oxygenated and more-oxygenated organic aerosols, respectively. This
332 proved that the increase in particle acidity simultaneously promoted the formation of
333 both less and more-oxygenated species, similar to that in the SO_2 experiments. However,
334 it is worth noting that higher acidity significantly promoted the chemical conversion of
335 less-oxygenated species (Factor 1) to more-oxygenated species (Factor 2) via
336 functionalization based on the comparison between the neutral and acidic seed particles
337 (Figure 4C). As shown in Figure 4B, the ion at m/z 114 ($C_6H_{10}O_2$) was assigned to
338 precursor-related ions. The highest ion signal fraction (m/z 114) in Factor 3 and the
339 similar mass spectrum between EM and Factor 3 in Figure S13 implied that Factor 3
340 represented precursor-related species (Figure 4C).

341 Based on the comparison of Factors between seed experiments and SO_2 , it should
342 be noted that Factor 1 and Factor 2 in the seed experiments differed from that in the
343 SO_2 experiment. For SO_2 experiments, acidity appeared to convert Factor 2 to Factor
344 1 after 200 minutes, but in seed experiments, the more H_2SO_4 caused the formation of
345 more Factor 2 and less Factor 1. Thus, we concluded that, for the same Factor in two
346 types of experiments, the corresponding composition should be different each other.
347 One possible explanation for this was that the increase in primary and secondary H_2SO_4
348 particles could also affect SOA composition to some extent, such as via changing the
349 reaction pathway of sCI.



350

351 **Figure 4.** Three-factor solutions for PMF analyses of SOA under different seed
 352 particles: (A) Time series of factor concentrations under acidic AAS; (B) Mass spectra
 353 of three factors; (C) Comparison of maximum concentration of two factors under
 354 neutral AS (black) and acidic AAS (red).

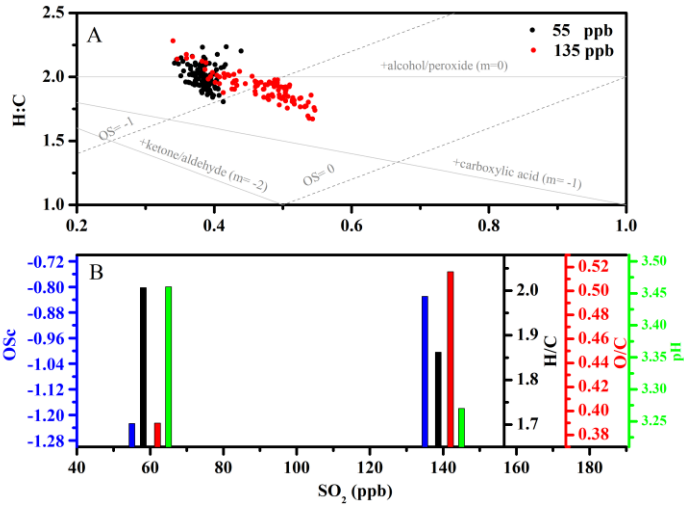
355 ***Elemental analysis in Van Krevelen diagrams***

356 The rate at which the H/C ratio changes with the O/C ratio in Van Krevelen
 357 diagrams can provide new information about the functional groups formed during
 358 oxidation (Chen et al., 2011; Lambe et al., 2012; Lambe et al., 2011; Li et al., 2019).
 359 As shown in Figure 5A and 6A, the average (H/C)/(O/C) slopes under different
 360 experimental conditions all approached -2. A slope of -2 is due to the formation of
 361 carbonyl species (Ng et al., 2011). This is consistent with the acknowledged reaction
 362 mechanism of alkene ozonolysis in the presence of SO₂, in which many carbonyl
 363 species and H₂SO₄ particles are produced (Newland et al., 2015a; Newland et al., 2015b;
 364 Sadezky et al., 2006; Sadezky et al., 2008). To verify whether increased OS_c was related
 365 to particle pH, particle pH was estimated using the E-AIM model (Model II: H⁺ – NH₄⁺
 366 – SO₄²⁻ – NO₃⁻ – H₂O) when secondary particle formation peaked under different SO₂
 367 concentrations (Hennigan et al., 2015; Peng et al., 2019). Since no organics are
 368 considered in Model II, there was an inherent assumption here that the acidity and the

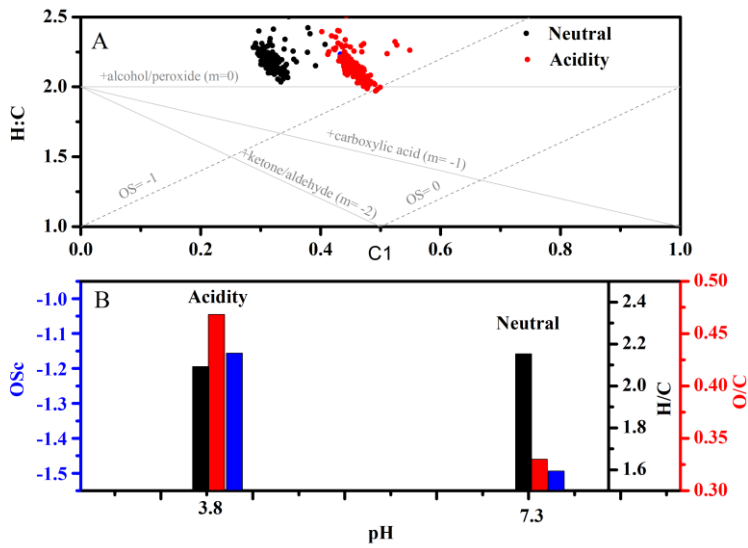
369 water uptake was dominated by the inorganic ions. From Figure 5B, the acidity for
370 nucleated H₂SO₄ particles (pH) under different SO₂ concentration have been estimated
371 to be 3.27 and 3.46, respectively. The acidities for AS and AAS (pH) have been
372 estimated to 7.3 and 4.1, respectively. The averaged oxidation state (OS_c) of SOA
373 increased with decreasing particulate pH in the absence of seeds. Similar trend was also
374 observed in the presence of seed particles (Figure 6B). This indicated that increased
375 OS_c was closely related to increased particles acidity either in the presence or absence
376 of seed particles. These results also indicated that both functionalization and
377 oligomerization associated with carbonyls groups dominate the formation of EM-
378 derived SOA. Moreover, it is worth noting that O/C increased when H/C decreased with
379 increased particle acidity in the absence of seed particles. In contrast, the O/C ratio
380 increased but the H/C ratio basically remained stable with increased particle acidity in
381 the presence of seed particles. These results implied that increased particle acidity
382 tended to promote the formation of more highly oxidized products via oligomerization
383 in the absence of seed particles and tended to promote the formation of more highly
384 oxidized products via functionalization in the presence of seed particles (Darer et al.,
385 2011; Shu et al., 2018; Zhang et al., 2019). However, the promoting contribution of
386 SOA functionalization conversion of total SOA could be ignored compared with the
387 reducing effect of acidic particles. Some studies showed that increased OS_c was closely
388 related to the formation of organosulfate (Liu et al., 2019a; Shu et al., 2018; Zhang et
389 al., 2019). To verify the organosulfate formation, the sulfate fragments along with S/C
390 ratio between AS and AAS experiments were also compared. As shown in Figure S17,
391 the similar S/C ratio and sulfate fragments distribution between neutral and acidic seed
392 experiments excluded the contribution of organosulfate formation to increased OS_c
393 (Chen et al., 2019c).
394

批注 [Peng21]: Reviewer 1: Specific comments Q10;
Reviewer 2: Specific comments Q4;

批注 [Peng22]: Reviewer 1: Specific comments Q14;



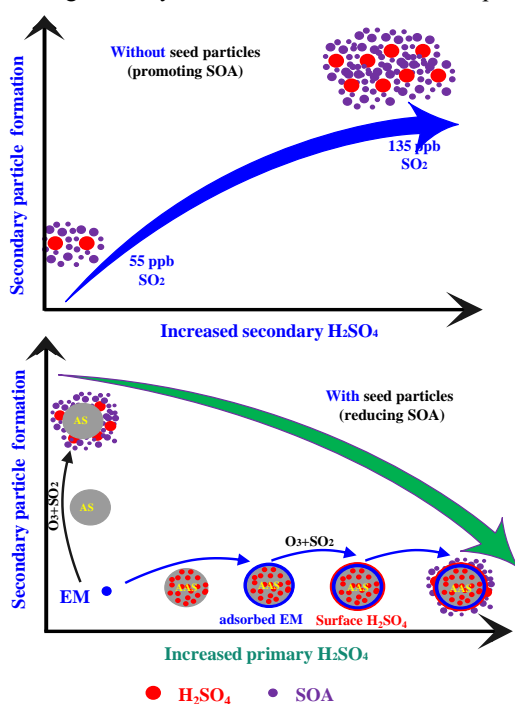
395
 396 **Figure 5.** Van Krevelen diagrams of elemental ratios under different initial
 397 concentrations of SO₂ (A); change in H/C ratio (black), O/C ratio (red), OS_c (blue), and
 398 particle pH (green) as a function of initial SO₂ concentration (B).



399
 400 **Figure 6.** Van Krevelen diagrams of elemental ratios under different seed particle
 401 acidity (A); change in H/C ratio (black), O/C ratio (red), and OS_c (blue) with particle
 402 acidity (B).

403 Taken together, in the absence of seed particles, the homogeneous formation of

404 more H₂SO₄ particles not only promoted the quick condensation of less- and more-
 405 oxygenated products and subsequent SOA formation via providing a greater surface
 406 area and volume, but enhanced the oligomerization process (Figure 7). In the presence
 407 of seed particles, the presence of more primary H₂SO₄ in seed particle enhanced EM
 408 uptake and functionalization process, but reduced SOA production due to the formation
 409 of surface H₂SO₄. This further indicated that the increase in primary and secondary
 410 H₂SO₄ particles could significantly affect SOA formation and composition.



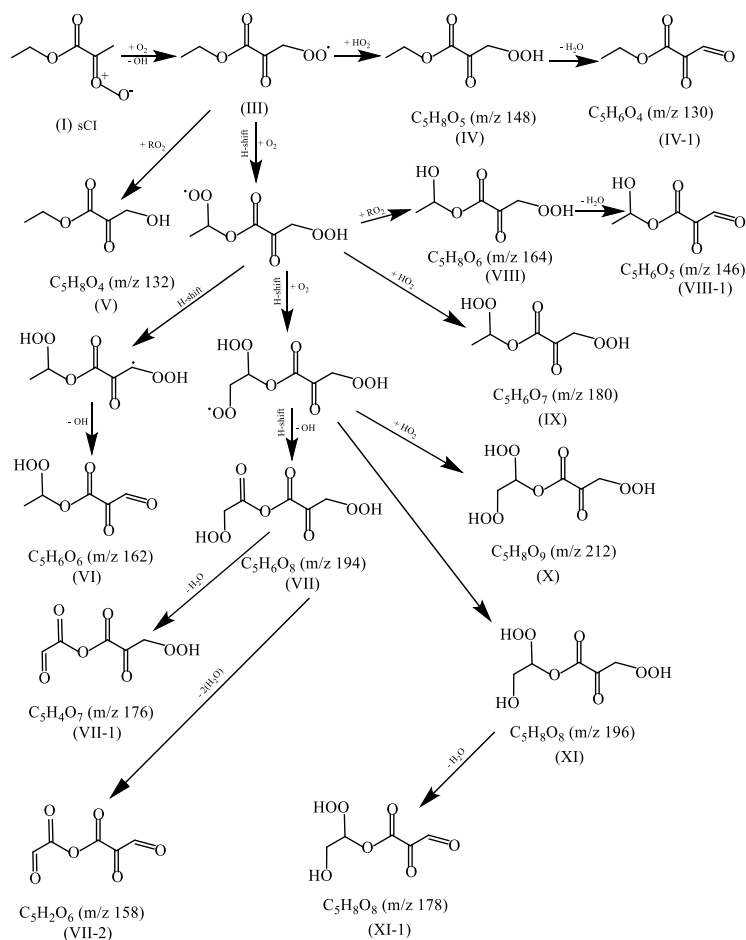
411
 412 **Figure 7.** Proposed the role of H₂SO₄ formation on EM-derived SOA

413
 414 **3.3. Reaction Mechanism of EM Ozonolysis**

415 In order to make clear the formation mechanism of EM-derived SOA, the
 416 evolutions of some molecular ion peaks have been checked in detail. As shown in
 417 Figure S18, the increase of their mass concentrations with reaction time indicated that
 418 these molecular ions peaks with m/z 116, 130, 132, 140, 146, 148, 158, 162, 164, 176,
 419 178, 180, 194, 196, and 212 should be the major ozonolysis products. Based on the

420 previously reported mechanism of alkene ozonolysis, the mechanism of EM ozonolysis
421 has been proposed in Scheme S1 (Jain et al., 2014; Vereecken and Francisco, 2012).
422 Briefly, oxidation of EM is initiated by addition of ozone across the double bond
423 resulting in a primary ozonide. The primary ozonide will produce two products
424 (formaldehyde and ketone ester) and two sCIs (sCI-1 and sCI-2). Based on the initial
425 carbonyl and sCI products (Scheme S1), it could be found that the saturated ketone ester
426 couldn't be further oxidized by O₃ and formaldehyde was the terminate products of sCI-
427 2 reaction. Thus, these major oxidation products observed in Figure S18 should come
428 from the further reaction of sCI-1. The mechanism of EM ozonolysis was proposed
429 based on previous studies (Bianchi et al., 2019; Jokinen et al., 2014; Newland et al.,
430 2018). Some highly oxidized multifunctional compounds could be produced via the H-
431 shift process including 1,7- and 1,8-H shift (Kurten et al., 2015; Mackenzie-Rae et al.,
432 2018). Thus, we concluded that the H-shift followed by autoxidation could be proposed
433 to be a formation pathway of highly oxidized multifunctional compounds.
434 Proposed reaction mechanism of sCI-1 was also shown in Scheme 1. These sCI-1 could
435 first convert to alkoxy radical (III) by losing OH group and O₂ addition. Then alkoxy
436 radical with an additional oxygen atom not only could further react with RO₂ to form
437 alcohols (V), but also react with HO₂ to form hydroperoxide product (IV). Moreover,
438 the intramolecular H-shift reaction may also compete with its bimolecular reaction with
439 HO₂ and other RO₂ radicals due to relatively weak C-H bonds in the molecule (Crouse
440 et al., 2013; Jokinen et al., 2014; Shu et al., 2018). Similarly, newly produced alkoxy
441 radical will continually and repeatedly react with HO₂, RO₂, and undergo its
442 intramolecular H-shift to form the higher oxidized alcohols, carbonyls, and
443 hydroperoxide product. The formation of these higher oxidized alcohols, carbonyls, and
444 hydroperoxide product might help to explain or give insight to the increased oxidation
445 state (OS_c) of the aerosol.

批注 [Peng23]: Reviewer 1: Specific comments Q12;



446

447 **Scheme 1.** Proposed mechanism for EM ozonolysis in the presence of AS particles

448

449 4. Conclusion

450 Some exposure measurement studies indicated that the concentration of ethyl
 451 methacrylate was notably higher than other methacrylate in the salons working air. The
 452 frequently exposure of methacrylate for a long time can trigger asthma or allergic
 453 contact dermatitis. Thus, the wide variety of sources and high volatility and toxicity of
 454 make EM a potential important source of environmental concern in the atmosphere. In
 455 China, O₃ pollution is gradually becoming serious environmental problem with the

456 decrease in PM_{2.5} concentration recent years. sCI, as a key reactive intermediate in
457 alkene ozonolysis, has been frequently reported to exhibit high oxidation capability in
458 the conversion of SO₂ and NO₂ to secondary particles (Newland et al., 2018). Thus,
459 investigating the ozonolysis of EM under complex condition help to evaluate their
460 potential contribution to haze formation.

批注 [Peng24]: Reviewer 1: Specific comments Q13;

461 In this work, we investigated and compared the formation of secondary particles
462 from EM ozonolysis under complex ambient condition. Results showed that a
463 substantial increase in secondary H₂SO₄ particles promoted SOA formation with
464 increasing SO₂. In contrast, the increase in primary H₂SO₄ proportion with seed acidity
465 enhanced EM uptake but reduced SOA formation. To clarify the underlying causes, we
466 analyzed the size distribution, chemical composition and evolution of SOA based on
467 PMF solutions and Van Krevelen diagrams. In the absence of seed particles, the
468 substantial increase in secondary H₂SO₄ particles with SO₂ provided greater surface
469 area and volume for further condensation of oxidation products. Moreover, enhanced
470 oligomerization functionalization of carbonyl species with increased particle acidity
471 also contributed to the increase in SOA in the absence of seed particles. However, in
472 the presence of seed particles, the increase of primary H₂SO₄ proportion in seed with
473 acidity enhanced more EM uptake, but the direct heterogeneous formation of H₂SO₄ on
474 the particle surface, differing from the condensation or nucleation of gas-phase H₂SO₄,
475 hampered the continuous heterogeneous ozonolysis of these adsorbed EM. Moreover,
476 even though increased particles acidity also caused chemical conversion of SOA via
477 functionalization, the contribution of the produced functionalized products to SOA
478 could be ignored due to the limited change in overall SOA formation. These results
479 indicated that the increase of primary and secondary H₂SO₄ particle has the different
480 effect on EM-derived SOA formation and its composition.

481 Taken together, our findings help to further understand the complicated effects of
482 increased H₂SO₄ components on SOA formation and composition during haze pollution.
483 However, more quantitative investigation based on a proton transfer reaction time-of-
484 flight mass spectrometry (PTR-TOFMS) and Nitrate ion chemical ionization mass

485 spectrometry (NO₃-CIMS) would be very necessary to accurately evaluate the
486 contribution of H₂SO₄ particles to SOA formation (yield) and composition (molecule
487 structure) in the future study. In addition to EM, many other unsaturated esters such as
488 methyl methacrylate (MA), butyl methacrylate (BMA), and propyl methacrylate (PMA)
489 are also frequently measured in the real atmosphere (Blanco et al., 2014; Ren et al.,
490 2019). Thus, more researches are needed to investigate the secondary particles potential
491 of these unsaturated esters, especially under complex ambient conditions, which will
492 help to further effectively evaluate the potential contribution of their atmospheric
493 oxidation process to secondary particle formation.

批注 [Peng25]: Reviewer 2: Specific comments Q13;
Reviewer 1: Specific comments Q3;

批注 [Peng26]: Reviewer 1: Specific comments Q13;

494

495 **Corresponding Author and Author Contributions**

496 * Phone: (+86)-010-62849508;

497 E-mail: qxma @rcees.ac.cn.

498 E-mail: bwchu @rcees.ac.cn.

499 PZ and TC designed and conducted this experiment, TC helped to analyze experimental
500 data. JL, XG, and WS gave assistance in measurements. HH, QM and BC discussed the
501 data results. PZ wrote the paper with input from all coauthors. All authors contributed
502 to the final paper.

503

504 **Notes**

505 The authors declare no competing financial interests.

506

507 **Acknowledgments**

508 This work was financially supported by the National Natural Science Foundation of
509 China (21976098, 22006152, 41605100, 41705134, 21876185, 91744205, and
510 41877304).

511

512 **References**

513 Arey, J., Winer, A. M., Atkinson, R., Aschmann, S. M., Long, W. D., and Morrison, C. L.: The Emission

514 of (Z)-3-Hexen-1-ol, (Z)-3-Hexenylacetate and Other Oxygenated Hydrocarbons from Agricultural
515 Plant-Species, *Atmos Environ a-Gen*, 25, 1063-1075, Doi 10.1016/0960-1686(91)90148-Z, 1991.

516 Bernard, F., Eglunent, G., Daele, V., and Mellouki, A.: Kinetics and products of gas-phase reactions of
517 ozone with methyl methacrylate, methyl acrylate, and ethyl acrylate, *J. Phys. Chem. A*, 114, 8376-8383,
518 10.1021/jp104451v, 2010.

519 Bianchi, F., Kurten, T., Riva, M., Mohr, C., Rissanen, M. P., Roldin, P., Berndt, T., Crouse, J. D.,
520 Wennberg, P. O., Mentel, T. F., Wildt, J., Junninen, H., Jokinen, T., Kulmala, M., Worsnop, D. R.,
521 Thornton, J. A., Donahue, N., Kjaergaard, H. G., and Ehn, M.: Highly Oxygenated Organic Molecules
522 (HOM) from Gas-Phase Autoxidation Involving Peroxy Radicals: A Key Contributor to Atmospheric
523 Aerosol, *Chem. Rev.*, 119, 3472-3509, 10.1021/acs.chemrev.8b00395, 2019.

524 Blanco, M. B., Bejan, I., Barnes, I., Wiesen, P., and Teruel, M. A.: FTIR product distribution study of the
525 Cl and OH initiated degradation of methyl acrylate at atmospheric pressure, *Environ. Sci. Technol.*, 44,
526 7031-7036, 10.1021/es101831r, 2010.

527 Blanco, M. B., Bejan, I., Barnes, I., Wiesen, P., and Teruel, M. A.: Products and mechanism of the
528 reactions of OH radicals and Cl atoms with methyl methacrylate ($\text{CH}_2=\text{C}(\text{CH}_3)\text{C}(\text{O})\text{OCH}_3$) in the
529 presence of NO_x, *Environ. Sci. Technol.*, 48, 1692-1699, 10.1021/es404771d, 2014.

530 Chen, Q., Liu, Y., Donahue, N. M., Shilling, J. E., and Martin, S. T.: Particle-phase chemistry of
531 secondary organic material: modeled compared to measured O:C and H:C elemental ratios provide
532 constraints, *Environ. Sci. Technol.*, 45, 4763-4770, 10.1021/es104398s, 2011.

533 Chen, T. Z., Liu, Y. C., Liu, C. G., Liu, J., Chu, B. W., and He, H.: Important role of aromatic
534 hydrocarbons in SOA formation from unburned gasoline vapor, *Atmos. Environ.*, 201, 101-109,
535 10.1016/j.atmosenv.2019.01.001, 2019a.

536 Chen, T. Z., Liu, Y. C., Ma, Q. X., Chu, B. W., Zhang, P., Liu, C. G., Liu, J., and He, H.: Significant
537 source of secondary aerosol: formation from gasoline evaporative emissions in the presence of SO₂ and
538 NH₃, *Atmos. Chem. Phys.*, 19, 8063-8081, 10.5194/acp-19-8063-2019, 2019b.

539 Chen, Y., Xu, L., Humphry, T., Hettiyadura, A. P. S., Ovadnevaite, J., Huang, S., Poulain, L., Schroder,
540 J. C., Campuzano-Jost, P., Jimenez, J. L., Herrmann, H., O'Dowd, C., Stone, E. A., and Ng, N. L.:
541 Response of the Aerodyne Aerosol Mass Spectrometer to Inorganic Sulfates and Organosulfur
542 Compounds: Applications in Field and Laboratory Measurements, *Environ. Sci. Technol.*, 53, 5176-5186,

543 10.1021/acs.est.9b00884, 2019c.

544 Chu, B. W., Zhang, X., Liu, Y. C., He, H., Sun, Y., Jiang, J. K., Li, J. H., and Hao, J. M.: Synergetic
545 formation of secondary inorganic and organic aerosol: effect of SO₂ and NH₃ on particle formation and
546 growth, *Atmos. Chem. Phys.*, 16, 14219-14230, 10.5194/acp-16-14219-2016, 2016.

547 Colomer, J. P., Blanco, M. B., Penenory, A. B., Barnes, I., Wiesen, P., and Teruel, M. A.: FTIR gas-phase
548 kinetic study on the reactions of OH radicals and Cl atoms with unsaturated esters: Methyl-3,3-dimethyl
549 acrylate, (E)-ethyl tiglate and methyl-3-butenolate, *Atmos. Environ.*, 79, 546-552,
550 10.1016/j.atmosenv.2013.07.009, 2013.

551 Crounse, J. D., Nielsen, L. B., Jorgensen, S., Kjaergaard, H. G., and Wennberg, P. O.: Autoxidation of
552 Organic Compounds in the Atmosphere, *J. Phys. Chem. Lett.*, 4, 3513-3520, 10.1021/jz4019207, 2013.

553 Darer, A. I., Cole-Filipiak, N. C., O'Connor, A. E., and Elrod, M. J.: Formation and stability of
554 atmospherically relevant isoprene-derived organosulfates and organonitrates, *Environ. Sci. Technol.*, 45,
555 1895-1902, 10.1021/es103797z, 2011.

556 Drewnick, F., Hings, S. S., DeCarlo, P., Jayne, J. T., Gonin, M., Fuhrer, K., Weimer, S., Jimenez, J. L.,
557 Demerjian, K. L., Borrmann, S., and Worsnop, D. R.: A new time-of-flight aerosol mass spectrometer
558 (TOF-AMS) - Instrument description and first field deployment, *Aerosol Sci. Technol.*, 39, 637-658,
559 10.1080/02786820500182040, 2005.

560 Foreman, E. S., Kapnas, K. M., and Murray, C.: Reactions between Criegee Intermediates and the
561 Inorganic Acids HCl and HNO₃: Kinetics and Atmospheric Implications, *Angew. Chem. Int. Ed. Engl.*,
562 55, 10419-10422, 10.1002/anie.201604662, 2016.

563 Friedman, B., Brophy, P., Brune, W. H., and Farmer, D. K.: Anthropogenic Sulfur perturbations on
564 biogenic oxidation: so₂ additions impact gas-phase oh oxidation products of alpha- and beta-pinene,
565 *Environ. Sci. Technol.*, 50, 1269-1279, 10.1021/acs.est.5b05010, 2016.

566 Gordon, T. D., Presto, A. A., May, A. A., Nguyen, N. T., Lipsky, E. M., Donahue, N. M., Gutierrez, A.,
567 Zhang, M., Maddox, C., Rieger, P., Chattopadhyay, S., Maldonado, H., Maricq, M. M., and Robinson, A.
568 L.: Secondary organic aerosol formation exceeds primary particulate matter emissions for light-duty
569 gasoline vehicles, *Atmos. Chem. Phys.*, 14, 4661-4678, 10.5194/acp-14-4661-2014, 2014.

570 Hamilton, J. F., Lewis, A. C., Carey, T. J., Wenger, J. C., Garcia, E. B. I., and Munoz, A.: Reactive
571 oxidation products promote secondary organic aerosol formation from green leaf volatiles, *Atmos. Chem.*

572 Phys., 9, 3815-3823, 10.5194/acp-9-3815-2009, 2009.

573 Han, Y. M., Stroud, C. A., Liggio, J., and Li, S. M.: The effect of particle acidity on secondary organic
574 aerosol formation from alpha-pinene photooxidation under atmospherically relevant conditions, *Atmos.*
575 *Chem. Phys.*, 16, 13929-13944, 10.5194/acp-16-13929-2016, 2016.

576 Harvey, R. M., Bateman, A. P., Jain, S., Li, Y. J., Martin, S., and Petrucci, G. A.: Optical Properties of
577 Secondary Organic Aerosol from cis-3-Hexenol and cis-3-Hexenyl Acetate: Effect of Chemical
578 Composition, Humidity, and Phase, *Environ. Sci. Technol.*, 50, 4997-5006, 10.1021/acs.est.6b00625,
579 2016.

580 Hennigan, C. J., Izumi, J., Sullivan, A. P., Weber, R. J., and Nenes, A.: A critical evaluation of proxy
581 methods used to estimate the acidity of atmospheric particles, *Atmos. Chem. Phys.*, 15, 2775-2790,
582 10.5194/acp-15-2775-2015, 2015.

583 Henriks-Eckerman, M. L., and Korva, M.: Exposure to airborne methacrylates in nail salons, *J. Occup.*
584 *Environ. Hyg.*, 9, D146-150, 10.1080/15459624.2012.696023, 2012.

585 Iinuma, Y., Boge, O., Gnauk, T., and Herrmann, H.: Aerosol-chamber study of the alpha-pinene/O₃
586 reaction: influence of particle acidity on aerosol yields and products, *Atmos. Environ.*, 38, 761-773,
587 10.1016/j.atmosenv.2003.10.015, 2004.

588 Jain, S., Zahardis, J., and Petrucci, G. A.: Soft ionization chemical analysis of secondary organic aerosol
589 from green leaf volatiles emitted by turf grass, *Environ. Sci. Technol.*, 48, 4835-4843,
590 10.1021/es405355d, 2014.

591 Jokinen, T., Sipila, M., Richters, S., Kerminen, V. M., Paasonen, P., Stratmann, F., Worsnop, D., Kulmala,
592 M., Ehn, M., Herrmann, H., and Berndt, T.: Rapid autoxidation forms highly oxidized RO₂ radicals in
593 the atmosphere, *Angew. Chem. Int. Ed. Engl.*, 53, 14596-14600, 10.1002/anie.201408566, 2014.

594 Konig, G., Brunda, M., Puxbaum, H., Hewitt, C. N., Duckham, S. C., and Rudolph, J.: Relative
595 contribution of oxygenated hydrocarbons to the total biogenic voc emissions of selected mid-european
596 agricultural and natural plant-species, *Atmos. Environ.*, 29, 861-874, Doi 10.1016/1352-2310(95)00026-
597 U, 1995.

598 Kristensen, K., Cui, T., Zhang, H., Gold, A., Glasius, M., and Surratt, J. D.: Dimers in alpha-pinene
599 secondary organic aerosol: effect of hydroxyl radical, ozone, relative humidity and aerosol acidity, *Atmos.*
600 *Chem. Phys.*, 14, 4201-4218, 10.5194/acp-14-4201-2014, 2014.

601 Kurten, T., Rissanen, M. P., Mackeprang, K., Thornton, J. A., Hyttinen, N., Jorgensen, S., Ehn, M., and
602 Kjaergaard, H. G.: Computational study of hydrogen shifts and ring-opening mechanisms in alpha-pinene
603 ozonolysis products, *J. Phys. Chem. A*, 119, 11366-11375, 10.1021/acs.jpca.5b08948, 2015.

604 Lambe, A. T., Onasch, T. B., Massoli, P., Croasdale, D. R., Wright, J. P., Ahern, A. T., Williams, L. R.,
605 Worsnop, D. R., Brune, W. H., and Davidovits, P.: Laboratory studies of the chemical composition and
606 cloud condensation nuclei (CCN) activity of secondary organic aerosol (SOA) and oxidized primary
607 organic aerosol (OPOA), *Atmos. Chem. Phys.*, 11, 8913-8928, 10.5194/acp-11-8913-2011, 2011.

608 Lambe, A. T., Onasch, T. B., Croasdale, D. R., Wright, J. P., Martin, A. T., Franklin, J. P., Massoli, P.,
609 Kroll, J. H., Canagaratna, M. R., Brune, W. H., Worsnop, D. R., and Davidovits, P.: Transitions from
610 functionalization to fragmentation reactions of laboratory secondary organic aerosol (SOA) generated
611 from the OH oxidation of alkane precursors, *Environ. Sci. Technol.*, 46, 5430-5437, 10.1021/es300274t,
612 2012.

613 Li, K., Liggio, J., Lee, P., Han, C., Liu, Q. F., and Li, S. M.: Secondary organic aerosol formation from
614 alpha-pinene, alkanes, and oil-sands-related precursors in a new oxidation flow reactor, *Atmos. Chem.*
615 *Phys.*, 19, 9715-9731, 10.5194/acp-19-9715-2019, 2019.

616 Lin, Y. H., Zhang, Z. F., Docherty, K. S., Zhang, H. F., Budisulistiorini, S. H., Rubitschun, C. L., Shaw,
617 S. L., Knipping, E. M., Edgerton, E. S., Kleindienst, T. E., Gold, A., and Surratt, J. D.: Isoprene
618 epoxydiols as precursors to secondary organic aerosol formation: acid-catalyzed reactive uptake studies
619 with authentic compounds, *Environ. Sci. Technol.*, 46, 250-258, 10.1021/es202554c, 2012.

620 Lin, Y. H., Knipping, E. M., Edgerton, E. S., Shaw, S. L., and Surratt, J. D.: Investigating the influences
621 of SO₂ and NH₃ levels on isoprene-derived secondary organic aerosol formation using conditional
622 sampling approaches, *Atmos. Chem. Phys.*, 13, 8457-8470, 10.5194/acp-13-8457-2013, 2013.

623 Liu, C. G., Chen, T. Z., Liu, Y. C., Liu, J., He, H., and Zhang, P.: Enhancement of secondary organic
624 aerosol formation and its oxidation state by SO₂ during photooxidation of 2-methoxyphenol, *Atmos.*
625 *Chem. Phys.*, 19, 2687-2700, 10.5194/acp-19-2687-2019, 2019a.

626 Liu, C. G., Liu, Y. C., Chen, T. Z., Liu, J., and He, H.: Rate constant and secondary organic aerosol
627 formation from the gas-phase reaction of eugenol with hydroxyl radicals, *Atmos. Chem. Phys.*, 19, 2001-
628 2013, 10.5194/acp-19-2001-2019, 2019b.

629 Liu, S. J., Jia, L., Xu, Y. F., Tsona, N. T., Ge, S. S., and Du, L.: Photooxidation of cyclohexene in the

630 presence of SO₂: SOA yield and chemical composition, *Atmos. Chem. Phys.*, 17, 13329-13343,
631 10.5194/acp-17-13329-2017, 2017.

632 Mackenzie-Rae, F. A., Wallis, H. J., Rickard, A. R., Pereira, K. L., Saunders, S. M., Wang, X. M., and
633 Hamilton, J. F.: Ozonolysis of alpha-phellandrene - Part 2: Compositional analysis of secondary organic
634 aerosol highlights the role of stabilised Criegee intermediates, *Atmos. Chem. Phys.*, 18, 4673-4693,
635 10.5194/acp-18-4673-2018, 2018.

636 McFiggans, G., Mentel, T. F., Wildt, J., Pullinen, I., Kang, S., Kleist, E., Schmitt, S., Springer, M.,
637 Tillmann, R., Wu, C., Zhao, D., Hallquist, M., Faxon, C., Le Breton, M., Hallquist, A. M., Simpson, D.,
638 Bergstrom, R., Jenkin, M. E., Ehn, M., Thornton, J. A., Alfarra, M. R., Bannan, T. J., Percival, C. J.,
639 Priestley, M., Topping, D., and Kiendler-Scharr, A.: Secondary organic aerosol reduced by mixture of
640 atmospheric vapours, *Nature*, 565, 587-593, 10.1038/s41586-018-0871-y, 2019.

641 Newland, M. J., Rickard, A. R., Alam, M. S., Vereecken, L., Munoz, A., Rodenas, M., and Bloss, W. J.:
642 Kinetics of stabilised Criegee intermediates derived from alkene ozonolysis: reactions with SO₂, H₂O
643 and decomposition under boundary layer conditions, *Phys. Chem. Chem. Phys.*, 17, 4076-4088,
644 10.1039/c4cp04186k, 2015a.

645 Newland, M. J., Rickard, A. R., Vereecken, L., Munoz, A., Rodenas, M., and Bloss, W. J.: Atmospheric
646 isoprene ozonolysis: impacts of stabilised Criegee intermediate reactions with SO₂, H₂O and dimethyl
647 sulfide, *Atmos. Chem. Phys.*, 15, 9521-9536, 10.5194/acp-15-9521-2015, 2015b.

648 Newland, M. J., Rickard, A. R., Sherwen, T., Evans, M. J., Vereecken, L., Munoz, A., Rodenas, M., and
649 Bloss, W. J.: The atmospheric impacts of monoterpene ozonolysis on global stabilised Criegee
650 intermediate budgets and SO₂ oxidation: experiment, theory and modelling, *Atmos. Chem. Phys.*, 18,
651 6095-6120, 10.5194/acp-18-6095-2018, 2018.

652 Ng, N. L., Canagaratna, M. R., Jimenez, J. L., Chhabra, P. S., Seinfeld, J. H., and Worsnop, D. R.:
653 Changes in organic aerosol composition with aging inferred from aerosol mass spectra, *Atmos. Chem.*
654 *Phys.*, 11, 6465-6474, 10.5194/acp-11-6465-2011, 2011.

655 Offenberg, J. H., Lewandowski, M., Edney, E. O., Kleindienst, T. E., and Jaoui, M.: Influence of aerosol
656 acidity on the formation of secondary organic aerosol from biogenic precursor hydrocarbons, *Environ.*
657 *Sci. Technol.*, 43, 7742-7747, 10.1021/es901538e, 2009.

658 Pankow, J. F., Luo, W. T., Bender, D. A., Isabelle, L. M., Hollingsworth, J. S., Chen, C., Asher, W. E.,

659 and Zogorski, J. S.: Concentrations and co-occurrence correlations of 88 volatile organic compounds
660 (VOCs) in the ambient air of 13 semi-rural to urban locations in the United States, *Atmos. Environ.*, 37,
661 5023-5046, 10.1016/j.atmosenv.2003.08.006, 2003.

662 Peng, X., Vasilakos, P., Nenes, A., Shi, G., Qian, Y., Shi, X., Xiao, Z., Chen, K., Feng, Y., and Russell,
663 A. G.: Detailed analysis of estimated ph, activity coefficients, and ion concentrations between the three
664 aerosol thermodynamic models, *Environ. Sci. Technol.*, 53, 8903-8913, 10.1021/acs.est.9b00181, 2019.

665 Ren, Y. G., Cai, M., Daele, V., and Mellouki, A.: Rate coefficients for the reactions of OH radical and
666 ozone with a series of unsaturated esters, *Atmos. Environ.*, 200, 243-253,
667 10.1016/j.atmosenv.2018.12.017, 2019.

668 Riva, M., Bell, D. M., Hansen, A. M., Drozd, G. T., Zhang, Z., Gold, A., Imre, D., Surratt, J. D., Glasius,
669 M., and Zelenyuk, A.: Effect of organic coatings, humidity and aerosol acidity on multiphase chemistry
670 of isoprene epoxydiols, *Environ. Sci. Technol.*, 50, 5580-5588, 10.1021/acs.est.5b06050, 2016.

671 Rivela, C. B., Blanco, M. B., and Teruel, M. A.: Atmospheric degradation of industrial fluorinated
672 acrylates and methacrylates with Cl atoms at atmospheric pressure and 298 K, *Atmos. Environ.*, 178,
673 206-213, 10.1016/j.atmosenv.2018.01.055, 2018.

674 Rodigast, M., Mutzel, A., and Herrmann, H.: A quantification method for heat-decomposable
675 methylglyoxal oligomers and its application on 1,3,5-trimethylbenzene SOA, *Atmos. Chem. Phys.*, 17,
676 3929-3943, 10.5194/acp-17-3929-2017, 2017.

677 Sadezky, A., Chaimbault, P., Mellouki, A., Rompp, A., Winterhalter, R., Le Bras, G., and Moortgat, G.
678 K.: Formation of secondary organic aerosol and oligomers from the ozonolysis of enol ethers, *Atmos.*
679 *Chem. Phys.*, 6, 5009-5024, DOI 10.5194/acp-6-5009-2006, 2006.

680 Sadezky, A., Winterhalter, R., Kanawati, B., Rompp, A., Spengler, B., Mellouki, A., Le Bras, G.,
681 Chaimbault, P., and Moortgat, G. K.: Oligomer formation during gas-phase ozonolysis of small alkenes
682 and enol ethers: new evidence for the central role of the Criegee Intermediate as oligomer chain unit,
683 *Atmos. Chem. Phys.*, 8, 2667-2699, DOI 10.5194/acp-8-2667-2008, 2008.

684 Salgado, M. S., Gallego-Iniesta, M. P., Martin, M. P., Tapia, A., and Cabanas, B.: Night-time atmospheric
685 chemistry of methacrylates, *Environ. Sci. Pollut. Res. Int.*, 18, 940-948, 10.1007/s11356-011-0448-x,
686 2011.

687 Shu, Y. J., Ji, J., Xu, Y., Deng, J. G., Huang, H. B., He, M., Leung, D. Y. C., Wu, M. Y., Liu, S. W., Liu,

688 S. L., Liu, G. Y., Xie, R. J., Feng, Q. Y., Zhan, Y. J., Fang, R. M., and Ye, X. G.: Promotional role of Mn
689 doping on catalytic oxidation of VOCs over mesoporous TiO₂ under vacuum ultraviolet (VUV)
690 irradiation, *Appl. Catal. B-Environ.*, 220, 78-87, 10.1016/j.apcatb.2017.08.019, 2018.

691 Sun, Y., Zhang, Q., Hu, J., Chen, J., and Wang, W.: Theoretical study for OH radical-initiated atmospheric
692 oxidation of ethyl acrylate, *Chemosphere*, 119, 626-633, 10.1016/j.chemosphere.2014.07.056, 2015.

693 Surratt, J. D., Chan, A. W., Eddingsaas, N. C., Chan, M., Loza, C. L., Kwan, A. J., Hersey, S. P., Flagan,
694 R. C., Wennberg, P. O., and Seinfeld, J. H.: Reactive intermediates revealed in secondary organic aerosol
695 formation from isoprene, *Proc. Natl. Acad. Sci. USA.*, 107, 6640-6645, 10.1073/pnas.091114107, 2010.

696 Taccone, R. A., Moreno, A., Colmenar, I., Salgado, S., Martin, M. P., and Cabanas, B.: Kinetic study of
697 the OH, NO₃ radicals and Cl atom initiated atmospheric photo-oxidation of Iso-propenyl methyl ether,
698 *Atmos. Environ.*, 127, 80-89, 10.1016/j.atmosenv.2015.12.033, 2016.

699 Teruel, M. A., Lopez, R. S. P., Barnes, I., and Blanco, M. B.: Night-time atmospheric degradation of a
700 series of butyl methacrylates, *Chem. Phys. Lett.*, 664, 205-212, 10.1016/j.cplett.2016.09.040, 2016.

701 Ulbrich, I. M., Canagaratna, M. R., Zhang, Q., Worsnop, D. R., and Jimenez, J. L.: Interpretation of
702 organic components from Positive Matrix Factorization of aerosol mass spectrometric data, *Atmos.*
703 *Chem. Phys.*, 9, 2891-2918, 10.5194/acp-9-2891-2009, 2009.

704 Vereecken, L., and Francisco, J. S.: Theoretical studies of atmospheric reaction mechanisms in the
705 troposphere, *Chem. Soc. Rev.*, 41, 6259-6293, 10.1039/c2cs35070j, 2012.

706 Wang, K., Ge, M. F., and Wang, W. G.: Kinetics of the gas-phase reactions of NO₃ radicals with ethyl
707 acrylate, n-butyl acrylate, methyl methacrylate and ethyl methacrylate, *Atmos. Environ.*, 44, 1847-1850,
708 10.1016/j.atmosenv.2010.02.039, 2010.

709 Wong, J. P., Lee, A. K., and Abbatt, J. P.: Impacts of sulfate seed acidity and water content on isoprene
710 secondary organic aerosol formation, *Environ. Sci. Technol.*, 49, 13215-13221, 10.1021/acs.est.5b02686,
711 2015.

712 Zhang, P., Chen, T., Liu, J., Liu, C., Ma, J., Ma, Q., Chu, B., and He, H.: Impacts of SO₂, Relative
713 humidity, and seed acidity on secondary organic aerosol formation in the ozonolysis of butyl vinyl ether,
714 *Environ. Sci. Technol.*, 53, 8845-8853, 10.1021/acs.est.9b02702, 2019.

715 Zhang, P., Chen, T., Liu, J., Chu, B., Ma, Q., Ma, J., and He, H.: Impacts of mixed gaseous and particulate
716 pollutants on secondary particle formation during ozonolysis of butyl vinyl ether, *Environ. Sci. Technol.*,

717 54, 3909-3919, 10.1021/acs.est.9b07650, 2020.

718 Zhang, Q., Alfarra, M. R., Worsnop, D. R., Allan, J. D., Coe, H., Canagaratna, M. R., and Jimenez, J. L.:

719 Deconvolution and quantification of hydrocarbon-like and oxygenated organic aerosols based on aerosol

720 mass spectrometry, *Environ. Sci. Technol.*, 39, 4938-4952, 10.1021/es048568l, 2005.

721 Zhang, X., Cappa, C. D., Jathar, S. H., McVay, R. C., Ensberg, J. J., Kleeman, M. J., and Seinfeld, J. H.:

722 Influence of vapor wall loss in laboratory chambers on yields of secondary organic aerosol, *Proc. Natl.*

723 *Acad. Sci. USA.*, 111, 5802-5807, 10.1073/pnas.1404727111, 2014.

724 Zhao, D. F., Schmitt, S. H., Wang, M. J., Acir, I. H., Tillmann, R., Tan, Z. F., Novelli, A., Fuchs, H.,

725 Pullinen, I., Wegener, R., Rohrer, F., Wildt, J., Kiendler-Scharr, A., Wahner, A., and Mentel, T. F.: Effects

726 of NO_x and SO₂ on the secondary organic aerosol formation from photooxidation of alpha-pinene and

727 limonene, *Atmos. Chem. Phys.*, 18, 1611-1628, 10.5194/acp-18-1611-2018, 2018.

728 Zhao, Y., Wingen, L. M., Perraud, V., Greaves, J., and Finlayson-Pitts, B. J.: Role of the reaction of

729 stabilized Criegee intermediates with peroxy radicals in particle formation and growth in air, *Phys. Chem.*

730 *Chem. Phys.*, 17, 12500-12514, 10.1039/c5cp01171j, 2015.

731